0013-7227/06/$15.00/0
Printed in U.S.A.

Endocrinology 147(5):2346–2356

doi: 10.1210/en.2005-0396

Ontogeny of Regeneration of β-Cells in the Neonatal Rat after Treatment with Streptozotocin

Sandra Thyssen, Edith Arany, and D. J. Hill

Lawson Health Research Institute, St. Joseph's Health Care (S.T., E.A., D.J.H.), and Departments of Medicine (E.A., D.J.H.), Physiology and Pharmacology (D.J.H.), and Pediatrics (D.J.H.), University of Western Ontario, London, Ontario, Canada N6A 4V2

We induced partial β-cell loss within the pancreas of neonatal rats using streptozotocin (STZ) to better characterize the mechanisms leading to β-cell regeneration postnatally. Rats were administered either STZ (70 mg/kg) or buffer alone on postnatal d 4, and the endocrine pancreas was examined between 4 and 40 d later. STZ-treated rats showed an approximately 60% loss of existing β-cells and a moderate hyperglycemia (<15 mM glucose), with levels returning to near-control values after 20 d. Within preexisting islets, there was increased cell proliferation in both insulin- and glucagon-positive cells at 8 d as well as α-cell hyperplasia. These were associated with increased pancreatic content and circulating levels of glucagon. Pancreatic levels of glucagon-like polypeptide-1 (GLP-1) were increased 8 d after STZ compared with control values, and the GLP-1/glucagon ratio changed in favor of GLP-1. Administration of a GLP-1 receptor antagonist, GLP-1-(9–39), resulted in decreased recovery of β-cells after STZ and worse glucose tolerance. Atypical glucagon-positive cells were found within islets that colocalized pancreatic duodenal homeobox-1 or glucose transporter-2. Pancreatic levels of insulin mRNA did not return to control values until 40 d after STZ. Insulin-positive cells were found after 8 d that colocalized glucagon and GLP-1. The model shows that the pancreas of the young rat can rapidly regenerate a loss of β-cells, and this is associated with hyperplasia of α-cells with an altered phenotype of increased GLP-1 synthesis. The target cells of GLP-1 probably include immature β-cells that coexpress proglucagon. (*Endocrinology* 147: 2346–2356, 2006)

REGENERATION OF pancreatic β-cell mass after either toxin- or autoimmune-mediated destruction is possible in the young rodent, but the extent of the recovery decreases with age and is incomplete in adult life. Similarly, there is histological evidence of islet cell neogenesis and regenerative response in children and adolescents with type 1 diabetes (1, 2). However, robust regeneration of endogenous β-cell mass was found in adult mice after induction by transplanted, marrow-derived, hemopoietic stem cells (3) and in nonobese diabetic mice after administration of splenocytes together with complete Freund's adjuvant (4). Although the latter was partially due to transdifferentiation of a splenocyte fraction into both pancreatic endocrine and duct cells, the ability of irradiated splenocytes to cause islet regeneration showed that this also involved induction of regeneration by endogenous mechanisms. The loss of regenerative capacity in the untreated pancreas with age after β-cell depletion, therefore, is caused by a paucity of one or more rate-limiting trophic stimuli and is potentially reversible.

Although the embryonic origins and development of islets of Langerhans have been extensively studied (5–7), it is not clear whether regeneration postnatally involves a recapitulation of these pathways or whether β-cells derive from different precursor populations. We and others have shown that the endocrine pancreas in the rat undergoes substantial remodeling between 1 and 4 wk of fetal life, involving a loss of β-cells due to developmental apoptosis and their replacement with newly derived β-cells, demonstrating a more mature phenotype of acute, glucose-sensitive insulin release (8, 9). We hypothesized that this period of natural developmental plasticity of β-cells would allow the identification of mechanisms for β-cell replacement after depletion with streptozotocin (STZ).

Islet cell development in the embryo occurs from the pancreatic duct epithelium and involves a sequence of expression of transcription factors, including pancreatic duodenal homeobox-1 (Pdx-1), neurogenin-3, and Nkx2.2 (5, 6). Differentiation of lineages leading to β- and α-cells is determined by the differential expression of Pax (paired box) 4 *vs.* Pax6. The exact nature of the endocrine embryological cell precursor in the pancreas is uncertain, although is appears to be neurogenin-3-positive (10, 11). Cells immunopositive for nestin and c-Kit are located adjacent to pancreatic ducts and within islets (12). Although these were originally thought to be endocrine cell precursors, they were subsequently shown through lineage tracing to be mesenchymal and more closely associated with endothelial cell formation and vascular remodeling (13, 14). However, they appear intimately connected to endocrine cell development. Herrera (15) used cell-targeted diphtheria toxin expression to specifically delete glucagon-, insulin-, and pancreatic polypeptide-expressing cells, and concluded that glucagon-positive cells were not precursors for β-cells. Studies with Cre-tagged cells showed that insulin- and glucagon-expressing cells derive from mutually exclusive cell populations, but both can derive from

First Published Online February 16, 2006

Abbreviations: GAPDH, Glyceraldehyde-3-phosphate dehydrogenase; Glut-2, glucose transporter-2; PC, prohormone convertase; PCNA, proliferating cell nuclear antigen; Pdx-1, pancreatic duodenal homeobox-1; STZ, streptozotocin.

***Endocrinology* is published monthly by The Endocrine Society (http://www.endo-society.org), the foremost professional society serving the endocrine community.**

TABLE 1. Characteristics of the primers used for real-time PCR using the SYBR Green technique

Primer name	Primer pair sequence (5′–3′)	Fragment size (bp)	Ct range	Ref. no.
Insulin	tca cac ctg gtg gaa gct c aca atg cca cgc ttc tgc	180 (Genomic: 679)	16–23	31
GLP-1 receptor	agt agt gtg ctc caa ggg cat aag aaa gtg cgt acc cca ccg	191	24–30	32
β-Actin	gcc cct ctg aac cct aag cat cac aat gcc agt ggt a	139 (Genomic: 603)	15–20	33

Pdx-1-positive cells (15, 16). Both insulin and glucagon precursors can express the pancreatic polypeptide gene, but somatostatin and insulin share more immediate precursors than either do with glucagon (17).

Despite an 8-fold increase in β-cell mass between 1 month of age and adulthood in the rat, the endogenous rate of DNA synthesis falls 5-fold by 3 months of age (18). Renewal of β-cells postnatally potentially originates from several sources. Increased β-cell mass after prolonged experimental hyperglycemia resulted from tubular foci of new islet development and the frequent appearance of individual insulin-positive cells within acinar tissue, suggestive of cellular transdifferentiation (19). Destruction of acinar tissue after pancreatic duct ligation results in hyperplasia of the pancreatic ducts and the appearance of new islets by neogenesis (20). After partial pancreatectomy, there is partial compensation by the expansion of remaining islets through either β-cell replication or the activation and differentiation of endogenous precursor cells (21). The model of STZ depletion of β-cells in the neonatal rat has been studied extensively (22–24) and has been shown to result in substantial β-cell replacement, although the animals are predisposed to glucose intolerance later in life. Near-complete removal of β-cells leads to partial replacement through the appearance of new islets, whereas subtotal destruction is followed by renewal from within the islets (17, 22–25). Cell lineage marking of β-cells in mice followed by partial pancreatectomy showed that new β-cells in the remaining organ derived almost exclusively from existing β-cells in adult life (26). However, there is also clear evidence of a scarce subpopulation of multipotent islet precursor cells resident in both ducts and islets of the adult mouse pancreas (27). We have used partial deletion of β-cells with STZ in the neonatal rat to better define the mechanisms by which regeneration of β-cells can occur in early life.

Materials and Methods

Materials

Mouse anti-proliferating cell nuclear antigen (anti-PCNA) antibody (1:750 dilution) was purchased from Sigma-Aldrich Corp. (St. Louis, MO). Goat antiglucagon-like polypeptide-1 (anti-GLP-1; C-17) antibody (1:250 dilution) was purchased from Santa Cruz Biotechnology, Inc. (Santa Cruz, CA), and mouse antiinsulin and antiglucagon (1:250 dilution) were obtained from Sigma-Aldrich Corp. Rabbit antiglucagon (1:250 dilution) was purchased from Santa Cruz Biotechnology, Inc. Rabbit anti-GLP-1 receptor (1:200 dilution) and guinea pig antiinsulin (1:250 dilution) were purchased from Abcam (Cambridge, MA), and rabbit antiglucose transporter-2 (anti-Glut-2; 1:500 dilution) was obtained from Biogenesis, Inc. (Kingston, Ontario, Canada). Rabbit anti-Pdx-1 (1:500 dilution) detecting predominantly nuclear protein was a gift from C. V. E. Wright (Vanderbilt University, Nashville, TN). Biotinylated goat antirabbit, horse antimouse, or donkey antigoat IgG (1:500 dilution) and avidin-labeled peroxidase were purchased from Vector Laboratories, Inc. (Burlington, Ontario, Canada). Alexa Fluor350 goat antirabbit, Alexa Fluor488 goat antimouse and antiguinea pig IgG, and Alexa Fluor555 goat antirabbit and antimouse IgG were purchased from Molecular Probes, Inc. (Eugene, OR). Tetramethylrhodamine isothiocyanate (rhodamine) rabbit antigoat IgG were purchased from Jackson ImmunoResearch Laboratories, Inc. (West Grove, PA). All secondary fluorescent antibodies were used at 1:200 dilutions for 1 h. For double or triple labeling using mouse, rabbit, and guinea pig antisera, the secondary antibody used to visualize them did not cross-react with the other species. GLP-1-(9–39) was obtained from American Peptide Co. (Sunnyvale, CA).

Animals

Timed pregnant Wistar rats were purchased from Charles River Laboratories, Inc. (Montréal, Canada) and were delivered to the animal care facility at Lawson Health Research Institute at 17 d gestation to allow for acclimatization before parturition. Access to water and standard rat chow was given *ad libitum*, and animals were provided with a 12-h dark, 12-h light cycle. Litters were reduced to 12 pups at birth. On d 4 of postnatal life, half the pups in each litter were given a single ip bolus injection of 70 mg/kg STZ (Sigma-Aldrich Corp.) freshly prepared in citrate buffer (pH 4.5). The remainder received a sham injection of vehicle only. In one series of animals, the pups were anesthetized the day after receiving STZ or sham injection with a mixture of ketamine (30 mg/ml) and xylazine (3 mg/ml; 1 μl/g body weight), a microosmotic pump (model 1002; Alzet Corp., Cupertino, CA) was located sc in the dorsal area, and the incision was closed. Pumps were preloaded with 0.182 mg GLP-1-(9–39) in 100 μl saline, which was calculated to release at a rate of 50 pmol/kg·min for 2 wk. Control animals received pumps loaded with saline alone. Glucose was monitored daily with a hand-held glucometer DEX-2 (Bayer, Inc., Toronto, Canada) by lancing the tail vein (2 μl blood). Body weight was recorded, and animals were killed every 2 d by decapitation (up to d 6 of age) or by CO_2 asphyxiation until d 20, then at 40 d. Animals with minipumps were killed after exhaustion of their contents on d 19. Pancreata were collected immediately and snap-frozen on liquid nitrogen or fixed for histology. Blood was collected, and serum was separated and stored at −20 C. Four to six pups from at least three separate litters were studied at each time point. Some animals receiving osmotic minipumps were subjected to a glucose tolerance test on postnatal d 28. A bolus of ip glucose (2 g/kg weight) was given after a 5-h fast, and blood was sampled from the tail vein for up to 2 h for glucose measurement.

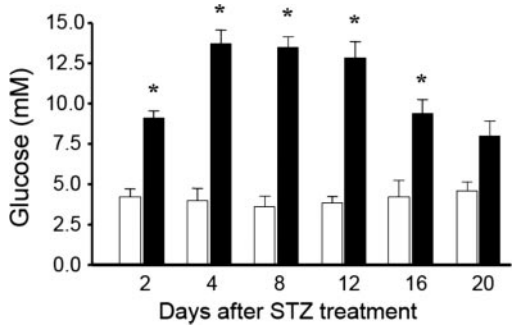

FIG. 1. Mean (±SEM) concentrations of fasting blood glucose in control animals (□) or animals treated with STZ (■) between 2 and 20 d after STZ treatment. Data are derived from 12–18 animals at each time point. *, $P < 0.05$ or better *vs.* control.

TABLE 2. Mean body and pancreatic weight in control and STZ-treated animals between 4 and 20 d after STZ treatment on postnatal d 4

	Days after STZ treatment				
	4	8	12	16	20
Body weight (g)					
Control	13.0 ± 0.5	25.1 ± 1.3	31.3 ± 1.2	36.5 ± 1.6	51.3 ± 2.9
STZ	12.0 ± 0.4	23.2 ± 1.2	27.1 ± 1.2	35.4 ± 1.7	45.4 ± 2.1
Pancreas weight (mg)					
Control	22 ± 3	53 ± 3	62 ± 4	84 ± 8	194 ± 10
STZ	18 ± 2	52 ± 3	60 ± 4	86 ± 7	170 ± 10

Data are the mean ± SEM (n = 3 litters; 18 animals).

Animal procedures were performed with the approval of the animal care committee of the University of Western Ontario in accordance with the guidelines provided by the Canadian Council for Animal Care.

Immunohistochemistry

Tissue was fixed in 10% neutral buffered formalin for 24–36 h and was embedded in paraffin. Sequential sections of 5 μm were cut and mounted on SuperFrost Plus glass slides (Fisher Scientific, Toronto, Canada). Immunohistochemistry was performed on pancreas sections to localize insulin and glucagon by a modified avidin-biotin peroxidase method (28). All antisera were diluted in 0.1 M PBS (pH 7.5) containing 0.25% (wt/vol) BSA, 0.3% (vol/vol) Triton X-100, and 0.01% (wt/vol) sodium azide (100 μl/slide). Slides were incubated for 24 h in a humidified chamber at 4 C. Biotinylated horse antimouse and goat antirabbit were used as secondary antibodies. Peptide immunoreactivity was localized by incubation in fresh diaminobenzidine tetrahydrochloride (Biogenex, San Ramon, CA). Tissue sections were counterstained with Carazzi's hematoxylin.

Dual staining for PCNA and glucagon was performed by first incubating with mouse anti-PCNA as described above. Signal amplification and visualization were accomplished by incubation in an avidin-biotin complex solution (Vectastain ABC Elite, Vector Laboratories, Inc., Burlingame, CA) and were visualized using alkaline phosphatase with blue reaction product (alkaline phosphatase substrate kit III, Vector Laboratories, Inc.) as the chromogen. Sections were then subjected to immunohistochemistry for glucagon as described above, using alkaline phosphatase with a red reaction product (Vector Laboratories, Inc.) as the chromogen. Sections were mounted under glass coverslips with an aqueous mounting solution.

For dual immunofluorescent localization of Pdx-1 and glucagon or of Glut-2 and glucagon, sections were deparaffinized and blocked with 10% (vol/vol) goat serum for 1 h at room temperature. After blotting, a mixture containing either rabbit anti-Pdx-1 or rabbit anti-Glut-2 and mouse antiglucagon antibody was added and incubated for 2 h at room temperature. After washing for 10 min in PBS, a mixture of the secondary antibodies, goat antimouse (Alexa 488) and antirabbit (Alexa 555), was added and incubated for 1 h at room temperature. Sections were washed in PBS for 10 min, covered with two or three drops of Prolong Antifade solution (Molecular Probes), and dried at room temperature before examination. GLP-1 and insulin were colocalized as described above by first blocking with 5% (vol/vol) rabbit serum and applying goat anti-GLP-1 antibody, followed by rabbit antigoat (tetramethylrhodamine isothiocyanate) secondary antibody. After 10 min of washing in PBS, the sections were blocked with 5% goat serum, and mouse antiinsulin antibody was applied, followed by goat antimouse (Alexa 488) secondary antibody. Glucagon, insulin, and the GLP-1 receptor were colocalized in a triple-immunofluorescence reaction as described above, except that the primary antiserum was rabbit anti-GLP-1 receptor; mouse antiglucagon and guinea pig antiinsulin were applied simultaneously and were detected with a mixture of goat antirabbit (Alexa 350), antimouse (Alexa 555), and antiguinea pig (Alexa 488) secondary antibodies.

Controls included substitution of primary antisera with nonimmune serum, omission of secondary antiserum, and, for insulin, glucagon, and GLP-1, absence of staining after preincubation of the antiserum with excess antigen. Briefly, the last positive dilution for each antiserum was determined, and the respective peptide was added at 5 times that molar concentration. After overnight incubation at 4 C, the antibody-peptide complex was centrifuged at 4 C at 14,000 rpm for 30 min, and the

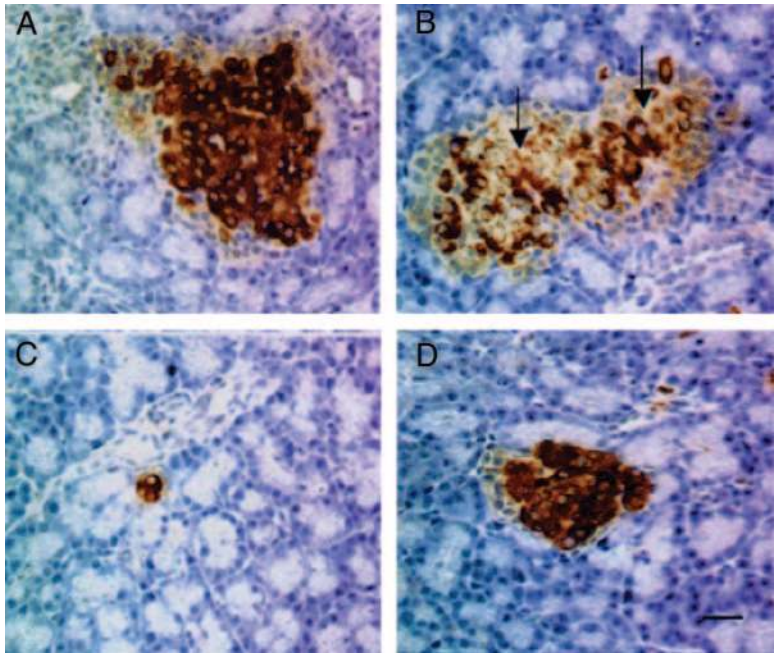

FIG. 2. Immunohistochemical localization of insulin in sections of rat pancreas, demonstrating islets in control (A) and STZ-treated (B) animals 4 d after treatment with STZ. The reduction in β-cell area was approximately 60%. Eight days after STZ treatment, increased numbers of small insulin-positive cell clusters were seen in association with pancreatic ducts (C); by 20 d, no evidence of remaining damage was apparent within islets (D). *Arrows* indicate β-cell loss after STZ. *Magnification bar*, 25 μm.

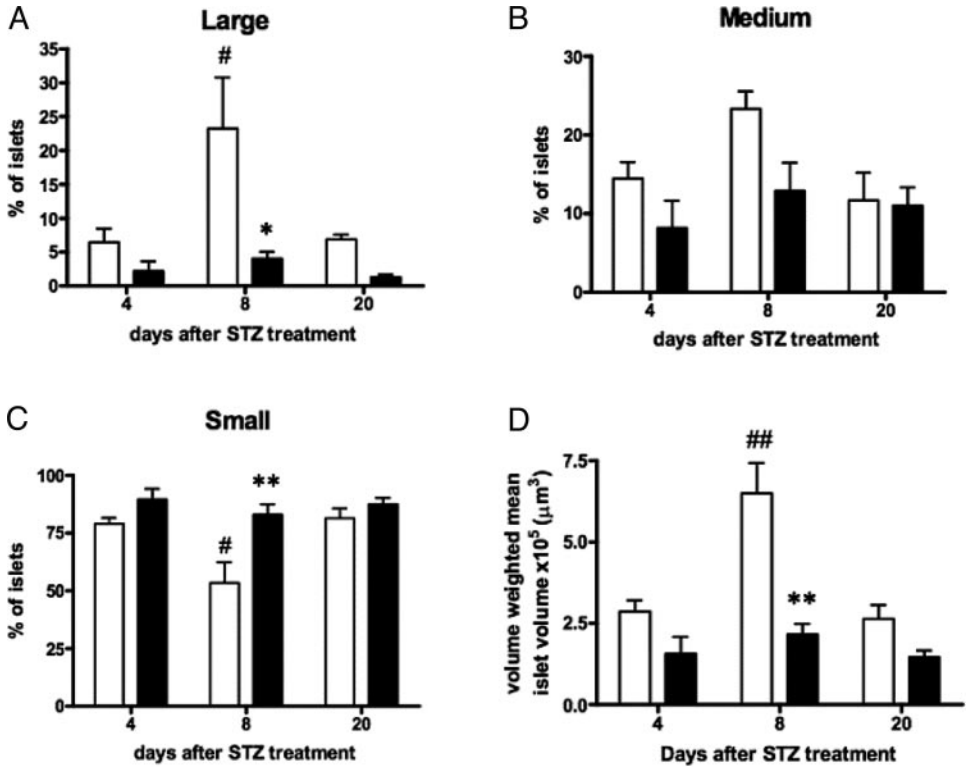

FIG. 3. Mean (±SEM) percentage of small (<5,000 μm^2), medium-sized (5,000–10,000 μm^2), or large (>10,000 μm^2) islets in pancreata of control animals (□) or animals treated with STZ (■; A–C) and mean weighted mean islet volume (D) at 4, 8, and 20 d after STZ treatment. Data represent 12–18 animals at each time point. *, $P < 0.05$; **, $P < 0.01$ (*vs.* control). #, $P < 0.05$; ##, $P < 0.01$ (*vs.* controls on d 4 and 20). Between 10 and 21 islets were analyzed for each tissue section.

supernatant was collected. An absence of signal using the supernatant as a first antibody indicated antibody specificity. The supernatant of antiserum without the blocking peptide was also collected as a positive control.

Morphometric analysis

Pancreata from at least three separate litters of rats representing between 12 and 18 animals were examined at each age for sham- and STZ-treated rats. Morphometric analysis was performed for three to five sections, representing different regions of the pancreas, using a transmitted light microscope (Carl Zeiss, Inc., New York, NY) at a magnification of ×250, ×400, or ×1000. Automatic image analysis of pancreatic sections for calculation of tissue areas was performed with Northern Eclipse (version 6.0) morphometric analysis software (Empix Imaging, Mississauga, Canada). The number of small (<5000 μm^2), large (>10,000 μm^2), or medium (5000–10,000 μm^2) islets and the percentage of islet cells immunoreactive for insulin, glucagon, or somatostatin were calculated for each group between 2 and 20 d after treatment. To estimate α-cell number, the total number of glucagon-immunoreactive cells per 10 mm^2 pancreas was calculated. The number of glucagon- or insulin-positive cells that also showed nuclear staining for PCNA was expressed as a percentage relative to the total number of each cell type within the same sections.

Pancreatic volume-weighted mean islet volumes were calculated as described by Bock *et al.* (29, 30). Volume-weighted mean islet volume represents the mean volume of islets weighted proportional to their volume and is considered a more accurate estimate than a simple number-weighted mean islet volume (29). This was calculated from:

$$Vv = \Sigma\pi/3 \times l_0^3$$

where Vv is the volume-weighted mean islet volume, and l_0 is the length of the line between the two intercepts of an islet and a horizontal line through a point grid that intercepts an islet (29).

RNA isolation and RT

Total RNA was isolated from entire frozen pancreas using TRIzol reagent (Invitrogen Life Technologies, Inc., Carlsbad, CA) and was additionally purified using the RNeasy 96-kit (QIAGEN, Valencia, CA) before being resuspended in diethylpyrocarbonate-treated distilled wa-

TABLE 3. Mean percentage of islet area occupied by cells immunopositive for insulin, glucagon, or somatostatin in control or STZ-treated animals between 2 and 20 d after STZ treatment on postnatal d 4

	Days after treatment					
	2	4	8	12	16	20
Insulin						
Control	67.5 ± 1.2	63.7 ± 0.8	63.6 ± 0.8	62.0 ± 3.8	64.2 ± 6.9	62.0 ± 2.7
STZ	44.5 ± 4.0[a]	45.1 ± 0.7	43.4 ± 0.2[a]	48.6 ± 6.7	63.0 ± 2.1	63.9 ± 1.4
Glucagon						
Control	22.9 ± 1.9	24.3 ± 1.0	22.1 ± 3.5	31.1 ± 1.3	25.5 ± 2.0	31.2 ± 2.5
STZ	35.1 ± 1.9[a]	29.4 ± 1.2	46.4 ± 3.4[a]	42.2 ± 3.5[a]	32.5 ± 0.7	33.7 ± 1.7
Somatostatin						
Control	3.8 ± 0.8	4.0 ± 0.7	5.3 ± 1.3	9.2 ± 0.8	10.4 ± 0.5	8.4 ± 0.6
STZ	5.1 ± 0.3	6.0 ± 0.7	12.0 ± 0.5[a]	7.7 ± 0.3	12.0 ± 0.7	12.3 ± 0.5[a]

Data are the mean ± SEM for tissue sections from 12–18 animals. Between eight and 17 islets were analyzed for each tissue section.
[a] $P < 0.05$ *vs.* control.

ter. RNA concentrations were determined from spectrophotometric absorption at 260 nm, and the ratio of absorbance at 260/280 nm was assessed to confirm purity (ratios >1.9). RT was performed using the Omniscript RT Kit (QIAGEN) following the manufacturer's instructions. Five micrograms of total RNA were reverse transcribed in a total volume of 50 μl using oligo(deoxythymidine) primers from Sigma-Genosys Corp. (Oakville, Canada). For every RT reaction set, one RNA sample was set up without reverse transcriptase enzyme to provide a negative control. Reactions were incubated at 25 C for 10 min, at 42 C for 50 min, and at 70 C for 15 min. After RT, samples were diluted by adding diethylpyrocarbonate-treated distilled water.

Real-time quantitative RT-PCR

Two different methods of real time PCR were performed. 1) Real-time quantitative PCR was performed using TaqMan probe technologies in an ABI PRISM 7900HT sequence detection system (Applied Biosystems, Foster City, CA) to determine the relative abundance of glucagon (Rn00562293-m1). Glyceraldehyde-3-phosphate dehydrogenase (GAPDH) mRNA was used as an endogenous control (TaqMan Rodent GAPDH Control Reagents, P/N: 4308313, Applied Biosystems). These primer probe sets span an intron for RNA specificity. PCRs were run in triplicate 50-μl reactions that contained 25 μl TaqMan Universal PCR Master Mix (P/N 4304437), 2.5 μl 20× Assays-on-Demand Gene Expression Assay Mix (Applied Biosystems), and 150 ng cDNA. Two-step PCR cycling was carried out as follows: one cycle of 50 C for 2 min, one cycle of 95 C 10 min, and 45 cycles of 95 C for 15 sec and 60 C for 1 min. 2) SYBR Green I quantitative real-time PCR was used to study the expression of insulin, GLP-1 receptor, and β-actin as an endogenous control. Gene-specific primers are shown in Table 1. All primers were purchased from Sigma-Genosys Corp. SYBR Green I Master Mix (QIAGEN) was used as recommended by the manufacturer [25 μl Master Mix, 2 μl primers (15 μM each), and 400 ng RT product in a total volume of 50 μl in triplicate]. Thermal cycling conditions were 15 min at 95 C, followed by 50 cycles of 15 sec at 95 C, 30 sec at 61.5, and 30 sec at 72 C, followed by a standard dissociation curve. The specificity of the SYBR Green I assay was verified by performing a melting curve analysis and by subsequencing the PCR products. The comparative threshold (CT) method (ΔΔCT method) was used, and validation experiments were performed to demonstrate that the efficiencies of target and reference genes were approximately equal (the plot of log input amount *vs.* ΔCT has a slope < 0.1). The threshold cycle range for proglucagon mRNA was 15–21; that for GAPDH mRNA was 20–28. These varied with the age of animal.

Hormone extraction and RIA

Frozen pancreata were weighed and homogenized twice in 2–3 ml 0.5% trifluoroacetic acid in a sonicator and left for 1 h at 4 C. Samples were rehomogenized and spun at 10,000 × *g*, and supernatants were stored at −20 C. Before the analysis, extracts were purified using Sep-Pak C_{18} (Waters Corp., Milford, MA) cartridges as previously described (34). Concentrations of glucagon or GLP-1 were measured in pancreatic extracts and serum by RIA (Linco Research, Inc., St. Charles, MO) following the manufacturer's instructions. Results were expressed as picomoles per milligram of pancreas. Assay sensitivities were 3 pM (9.89 pg/ml) for GLP-1 and 5.74 pM (20 pg/ml) for glucagon. Intra- and interassay coefficients of variation for GLP-1 were 26.5% and 26.7%, respectively; those for glucagon were 4.9% and 11.7%. Addition of up to 10 μM glucagon in the assay for GLP-1 caused no displacement of tracer.

Statistical analysis

Data are represented as the mean ± SEM and were compared using Student's *t* test or two-way ANOVA to assess the statistical significance between time courses, followed by a Bonferroni posttest when interaction was present. Significance was set at $P < 0.05$. All calculations were performed using PRISM version 4 (GraphPad, Inc., San Diego, CA) for Windows (Microsoft Corp., Redmond, WA).

Results

In animals receiving STZ, blood glucose levels were significantly elevated within 2 d of treatment compared with control animals and reached a plateau of approximately 13 mM between d 4 and 12 (Fig. 1). By d 20 after STZ treatment, blood glucose levels did not differ significantly from those in control rats, which remained euglycemic throughout the

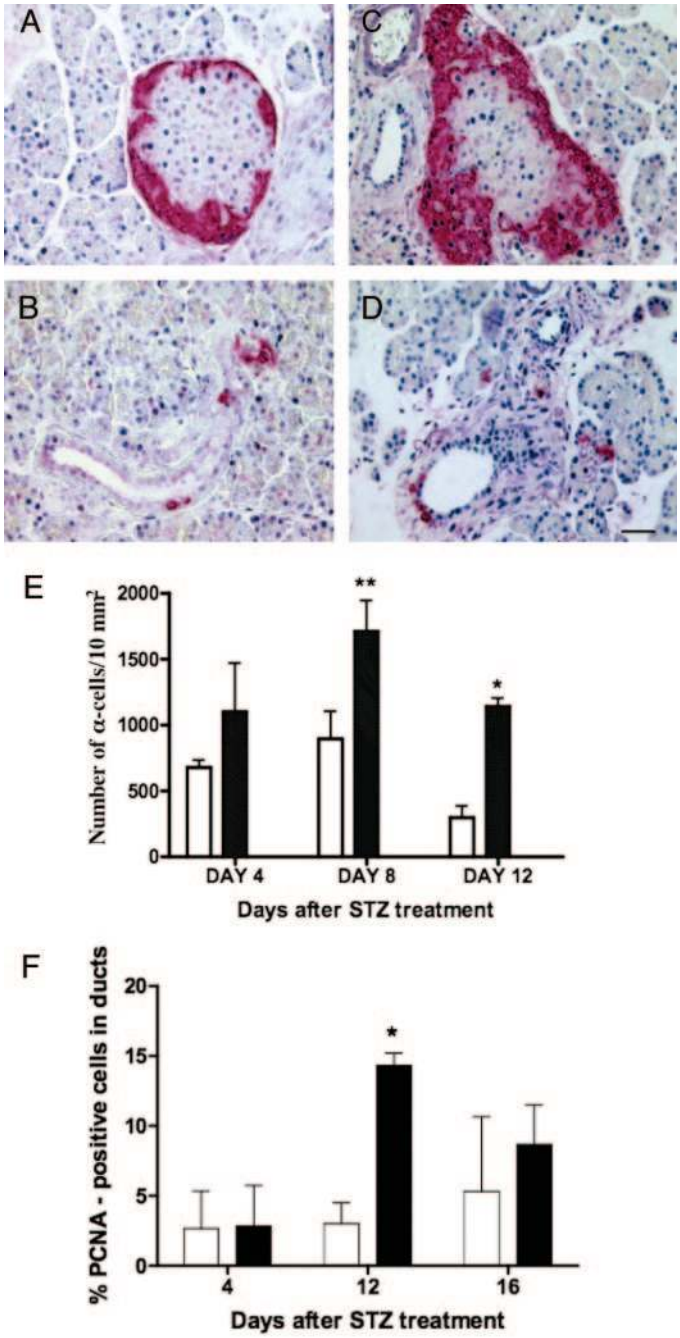

FIG. 4. A, Immunohistochemical localization of glucagon (*red*) and PCNA (*blue*) in sections of rat pancreas from control animals (A and B) or 8 d after STZ treatment (C and D). Representative islets are shown in A and C, and pancreatic ducts are shown in B and D. Magnification *bar*, 20 μm. E, Number (mean ± SEM) of α-cells per 10 mm^2 pancreas in control (□) *vs.* STZ-treated (■) animals 4, 8, and 12 d after treatment. F, Percentage of pancreatic ductal epithelial cells that costained for PCNA at 4, 12, and 16 d after STZ treatment. Data represent 12–18 animals at each time point. *, $P < 0.05$; **, $P < 0.01$ (*vs.* control).

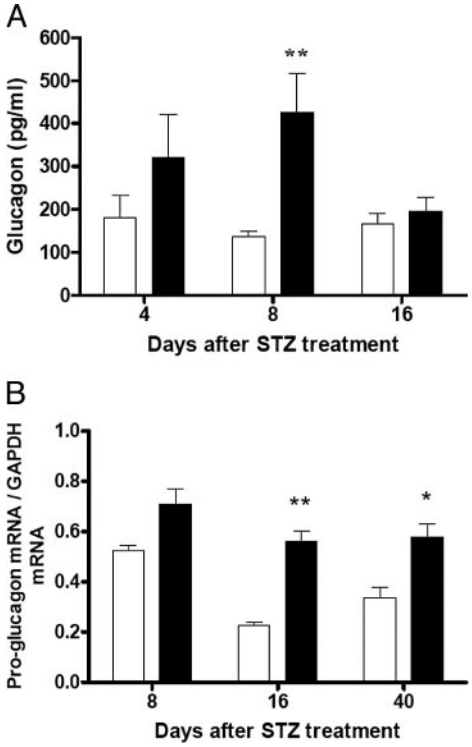

FIG. 5. Glucagon content in serum (A) and the ratio of mRNA encoding proglucagon (B) relative to GAPDH (mean ± SEM) in pancreata from control animals (□) or 8, 16, and 40 d after STZ treatment (■). Data represent 12–18 animals at each time point. *, $P < 0.05$; **, $P < 0.01$ (*vs.* control).

study. Treatment with STZ did not significantly alter mean body weight, pancreatic weight (Table 2), or liver weight (data not shown) compared with controls at any time point, and no mortality occurred.

Histological analysis showed that approximately 60% of insulin-immunoreactive cells within islets were lost after STZ treatment (Fig. 2). Four days after treatment, an increased number of small clusters of insulin-immunoreactive cells were seen adjacent to pancreatic ducts; by d 8, increased numbers of small islets were present without evidence of STZ-induced β-cell destruction. Between d 20 and 40 after STZ, the larger islets that had originally exhibited β-cell loss had now remodeled with a uniform core of insulin-positive β-cells. Calculation of the volume-weighted mean islet volume over the study period in control animals showed a substantial increase between 4 and 8 d (8 and 12 d age), with a decline between d 8 and 20, presumably associated with maturation and expansion of the exocrine tissue compartment. In animals receiving STZ, there was a 66% reduction in mean islet volume *vs.* controls on d 8 (Fig. 3D). When the percentages of small (<5000 μm^2), medium-sized (5000–10,000 μm^2), or large (>10,000 μm^2) islets were compared, the pancreata from STZ-treated animals had a significantly increased percentage of smaller islets compared with controls on d 8 after treatment, whereas the relative percentage of larger islets was much reduced (Fig. 3, A–C).

We subsequently determined how the relative volumes of islet endocrine cell types had changed to account for the reduced mean islet volume after STZ treatment. As expected,

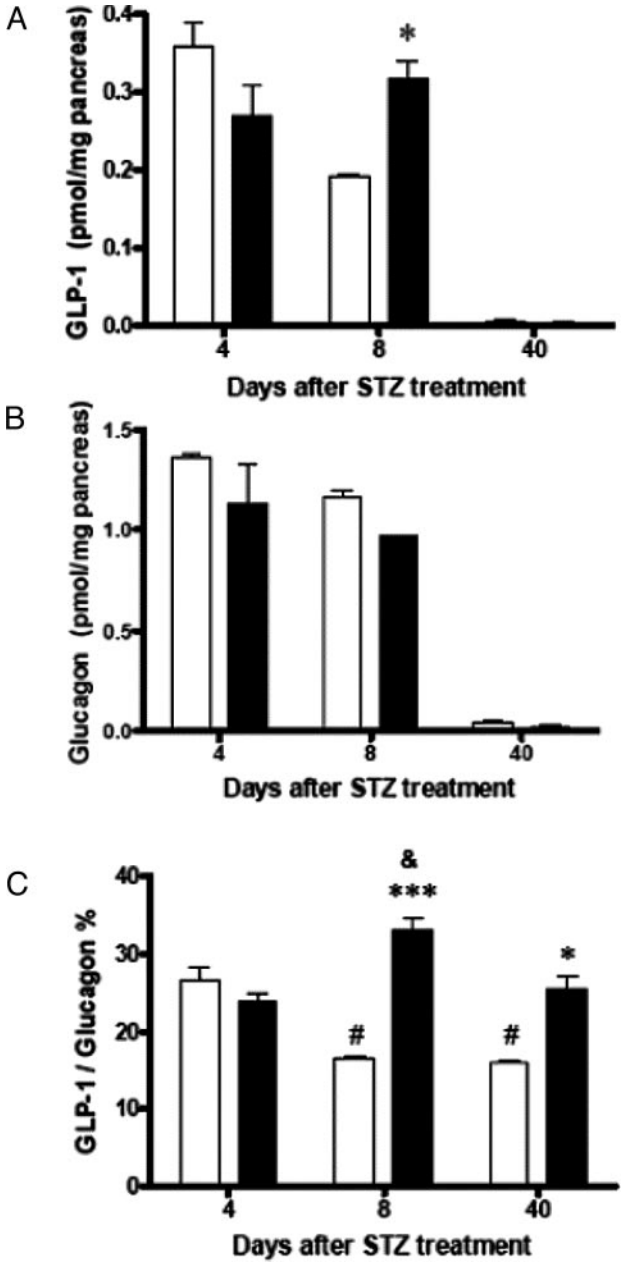

FIG. 6. Pancreatic content (mean ± SEM) of immunoreactive GLP-1 (A) or glucagon (B) and percentage of GLP-1/glucagon (C) in tissue from control animals (□) or 4, 8, and 40 d after STZ treatment (■). Data represent 12–18 animals at each time point. *, $P < 0.05$; ***, $P < 0.001$ (*vs.* control). #, $P < 0.05$ (*vs.* control on d 4). &, $P < 0.05$ (*vs.* STZ group on d 4).

there was a significant reduction in the mean area of islets accounted for by β-cells, and this resulted in a greater relative area accounted for by glucagon- or somatostatin-immunoreactive cells (Table 3). However, between 8 and 14 d after treatment, the area occupied by glucagon-positive cells increased sharply, as did the presence of somatostatin-containing cells on d 8. Dual immunohistological staining for both glucagon and PCNA confirmed an increased presence of α-cells with evidence of DNA synthesis 8 d after STZ treatment compared with control rats (Fig. 4A). When quan-

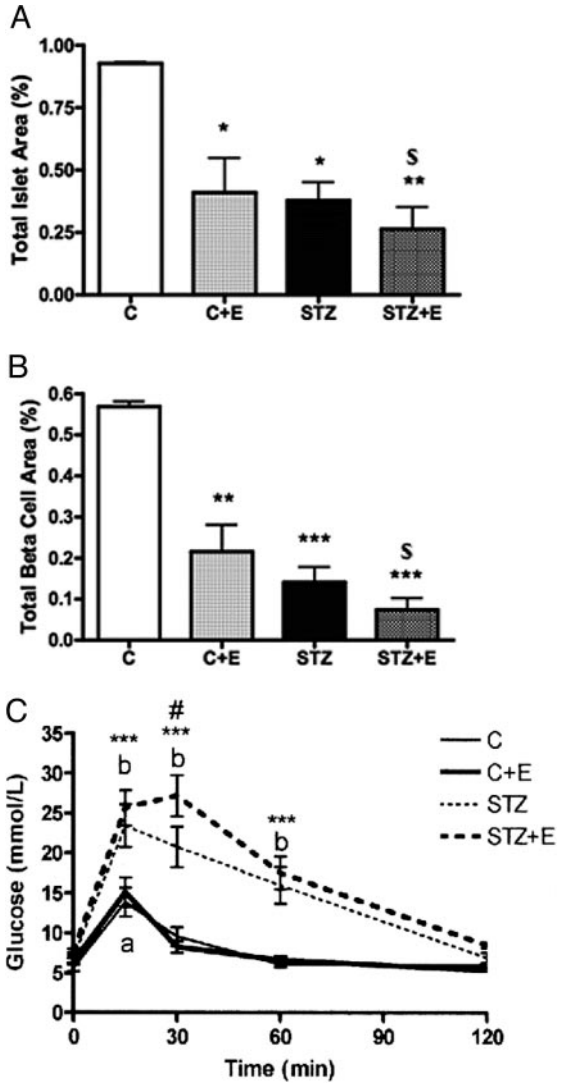

FIG. 7. Percent area of pancreas (mean ± SEM) occupied by total islet area (A) or β-cells (B) in animals that received saline alone (□), saline with GLP-1-(9–39) (▨), STZ (■), or STZ and GLP-1-(9–39) (▩). Figures represent eight to 10 animals at each time point. *, $P < 0.05$; **, $P < 0.01$; ***, $P < 0.001$ (*vs.* control). &, $P < 0.05$ (*vs.* STZ). C, Glucose values (mean ± SEM) during a glucose tolerance test in animals that had received saline (□), saline+GLP-1-(9–39) (▨), STZ (■), or STZ and GLP-1-(9–39) (▩). Data represent five rats at each time point. ***, $P < 0.001$ [STZ and STZ plus GLP-1-(9–39) *vs.* control or control and GLP-1-(9–39)]. #, $P < 0.05$ [STZ *vs.* STZ and GLP-1-(9–39]. a, $P < 0.01$ [control *vs.* control and GLP-1-(9–39)]. b, $P < 0.01$ [STZ or STZ and GLP-1-(9–39) *vs.* time zero].

tified, the number of α-cells per area of pancreas was significantly increased 8 and 12 d after STZ compared with controls (Fig. 4B). On d 8, the percentage of these α-cells that also showed nuclear staining for PCNA was 23 ± 2% in control animals, but it was 41 ± 3% was STZ treatment ($P < 0.01$). Within the same tissue sections, the percentage of β-cells that also stained for PCNA was 16 ± 3% in controls and 25 ± 4% after STZ ($P < 0.05$). PCNA labeling was also seen within ductal epithelial cells and was significantly increased in pancreas from STZ-treated rats on 12 d (Fig. 4C).

We examined the implications of an increased α-cell presence on the expression of the proglucagon gene and the

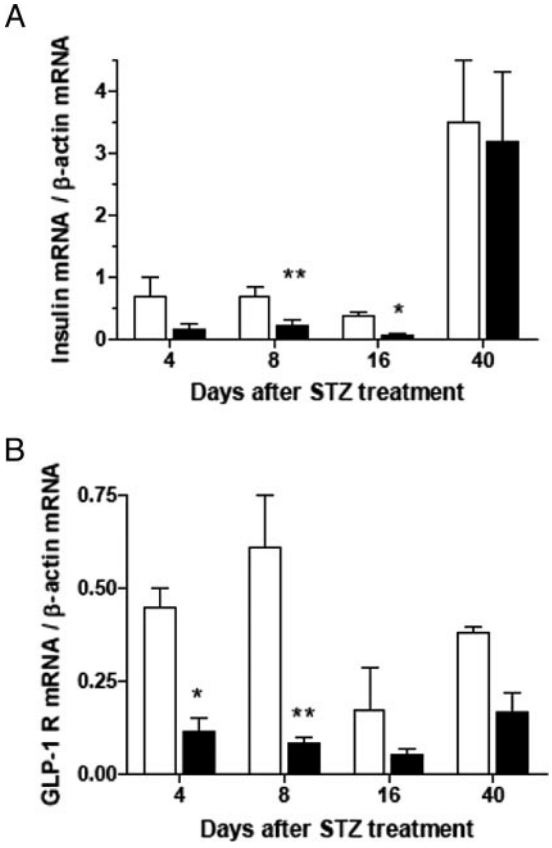

FIG. 8. Ratio of mRNAs encoding insulin (A) or GLP-1 receptor (B) relative to β-actin (mean ± SEM) in pancreata from control animals (□) or 4–40 d after STZ treatment (■). Data represent 12–18 animals at each time point. *, $P < 0.05$; **, $P < 0.001$ (*vs.* control).

presence of its products. Circulating glucagon was increased 8 d after STZ treatment, but was no different from control values on d 16 (Fig. 5A). Proglucagon mRNA was quantified by real-time PCR in intact pancreas and was significantly greater in STZ-treated animals between 16 and 40 d (Fig. 5B). The discrepancy between gene expression and circulating glucagon levels prompted the measurement of a second major product of the proglucagon gene, GLP-1. Glucagon and GLP-1 levels were each measured by RIA in extracts from intact pancreata. Both were present on d 4 and 8 after STZ treatment and declined by d 40 (Fig. 6). On d 8, the content of GLP-1 was significantly elevated in STZ-treated animals, whereas that of glucagon was unaltered, resulting in a significant change in the proglucagon gene product ratio in favor of GLP-1.

To examine the functional significance of increased GLP-1 synthesis, we administered the GLP-1 receptor antagonist, GLP-1-(9–39), to rats after saline or STZ treatment. These experiments were terminated on d 19, when the capacity of the minipumps was exhausted and before a full renewal of β-cells could be expected after STZ treatment. GLP-1-(9–39) treatment did not alter weight gain in these animals or have any visible deleterious effect. GLP-1-(9–39) alone caused a significant reduction in the mean islet area compared with controls (Fig. 7A) and in the area of pancreas represented by β-cells (Fig. 7B); this was reduced further in STZ-treated

animals. Some animals were followed until 28 d of age and subjected to a glucose tolerance test. GLP-1-(9–39) alone did not alter the glucose excursion profile, but animals receiving STZ had a significantly worse glucose tolerance if they had also received GLP-1-(9–39) (Fig. 7C).

Quantification of insulin mRNA showed that this continued to be lower than in control animals until at least d 16, but had returned to control values by d 40 after STZ (Fig. 8A). Similarly, mRNA for the GLP-1 receptor, which is present on β-cells, was also less abundant (Fig. 8B). Visualization of insulin-positive cells within islets of control rats by immunofluorescence on d 8 showed little costaining with GLP-1 or glucagon (Fig. 9), although they did contain the GLP-1 receptor (Fig. 10). However, in pancreata from animals receiving STZ, costaining of insulin with GLP-1 and glucagon was seen (Figs. 9 and 10), especially in small and medium-sized islets, at more than twice the frequency in control rats (Fig. 11). Islet cells from STZ-treated rats, but not controls, also demonstrated colocalization of glucagon with Pdx-1 and of glucagon with Glut-2 (Fig. 12).

Discussion

Developmental remodeling in the neonatal rat pancreas results in a relative reduction in β-cell mass relative to body weight at 2 wk of age, which is largely recovered by weaning (8). The induction of an approximately 60% loss of β-cells at this time using STZ was followed by the recovery of β-cell volume between 20 and 40 d later. Although the model resulted in transient hyperglycemia, no differences in mean body or pancreatic weight were seen compared with control animals. However, measurement of pancreatic insulin mRNA showed that this was substantially lower in STZ-treated rats on d 16 and had not recovered until d 40, suggesting that the recovered β-cell mass seen at 16 d after STZ treatment was not functionally mature. Nevertheless, the model demonstrates that an exaggeration of the developmental turnover of β-cells with STZ in neonatal life, with a 60% loss, is largely reversible within 5 wk. The ability to rapidly regenerate islet mass may be partly explained by the moderate and transient nature of the associated hyperglycemia. Prevention of hyperglycemia with insulin therapy in more severe models of STZ-induced cell loss resulted in a more rapid recovery of β-cell mass (23, 25).

Loss of β-cells was rapidly followed by the increased appearance of individual insulin- and glucagon-positive cells associated with pancreatic ducts, although increased labeling of duct epithelium with PCNA was not seen until d 12. This suggests that new endocrine cells appearing within the first 4 d after STZ treatment were derived directly from existing precursors within the ducts. By d 8 after treatment, there was a significantly increased population of smaller islets. This occurred despite a substantial reduction in total volume-weighted mean islet volume and a reduction in the number of larger islets subsequent to β-cell destruction, and it agrees with the islet neogenic activity reported previously after STZ treatment (35–37). However, a second likely source of new

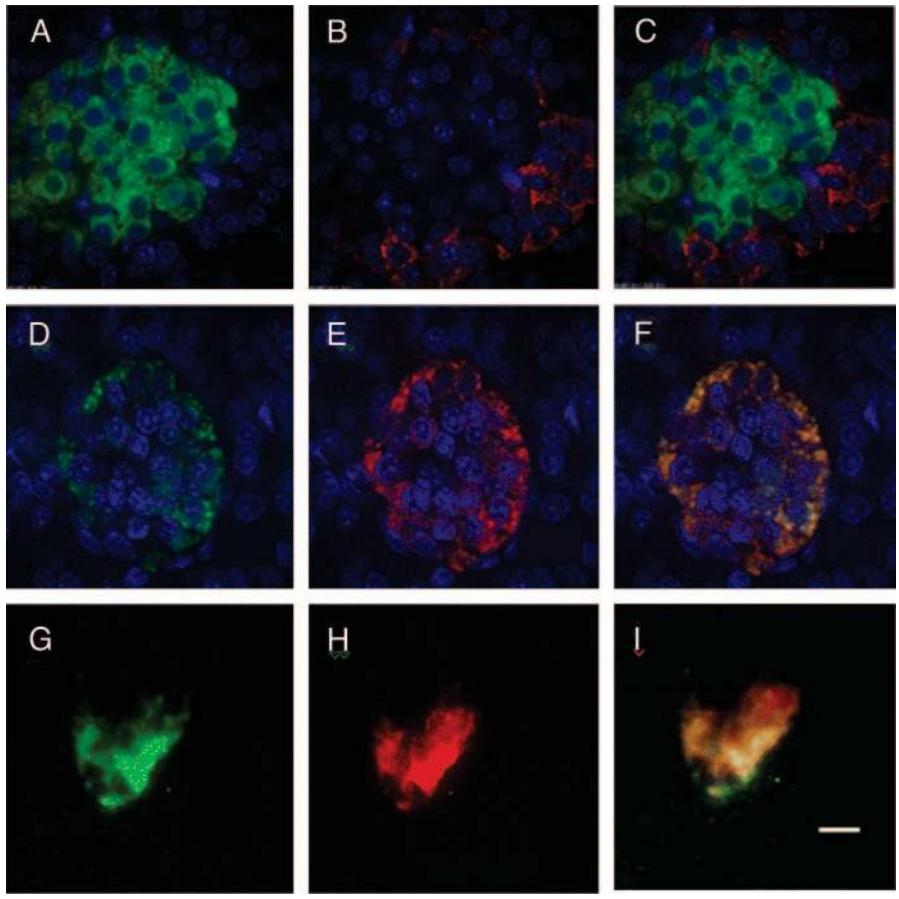

FIG. 9. Immunofluorescent colocalization of insulin (A), GLP-1 (B), and their superimposition (C) and of glucagon (D), GLP-1 (E), and their superimposition (F) in sections from the same islets from control animals (A–F). Insulin (G), GLP-1 (H), and their superimposition (I) are also shown for an animal 8 d after treatment with STZ (G–I). Magnification *bar*, 10 μm.

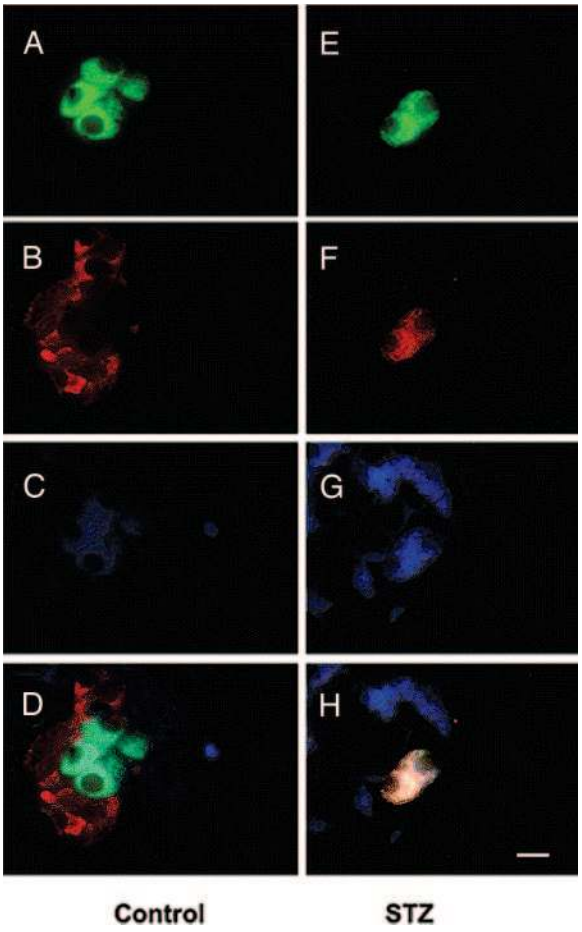

FIG. 10. Immunofluorescent colocalization of insulin (A and E), glucagon (B and F), GLP-1 receptor (C and G), and their superimposition (D and H) in the same histological sections from control animals (A–D) or animals 8 d after treatment with STZ (E–H). Magnification *bar*, 10 μm.

β-cells was from within existing islets. By 8 d after STZ treatment, an increased frequency of PCNA staining was seen in both glucagon- and insulin-positive cells. The increase in proliferative activity in glucagon-positive cells coincided with a significant increase in numbers on d 8 and 12. Hyperglycemia and reduced insulin availability are known to cause increased proglucagon gene expression and circulating glucagon (38, 39), but α-cell hyperplasia has only previously been reported in extreme models of glucagon loss, such as with deletion of the prohormone convertase-2 (PC2) gene (40). Some α-cells showed colocalization of glucagon with either Pdx-1 or Glut2, suggesting the appearance of an immature phenotype of α-cell. However, the major feature of this phenotype was a relative shift in proglucagon gene processing toward GLP-1.

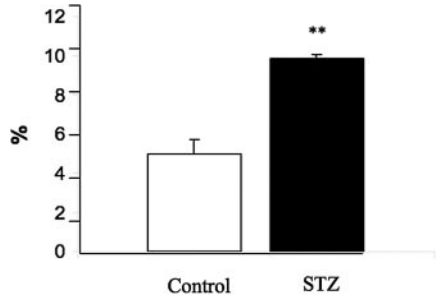

FIG. 11. Percentage of cells within islets showing immunofluorescent colocalization of insulin and GLP-1 from control animals or those treated with STZ, 8 d after treatment. Values show the mean ± SEM (n = 18 animals). **, $P < 0.01$ *vs.* control.

GLP-1 has a variety of trophic effects on β-cells, including enhancement of glucose-stimulated insulin release, stimulation of cell replication, inhibition of cytokine-mediated apoptosis, and ability to promote the replication and differentiation of β-cell progenitors (41–43). A homeostatic increase in islet-derived GLP-1 in juxtaposition to β-cells in damaged islets would be ideally placed to enable β-cell renewal by increased proliferation of existing cells or from resident precursors. Such a shift in gene product would imply a change in the expression of PCs within α-cells. All islet endocrine cell types express PC1/3, whereas α-cells express mainly PC2 (44). PC1/3 and PC2 act together at the β-cell to process proinsulin to insulin, whereas PC2 selectively converts proglucagon to glucagon in the α-cell. In intestinal L cells, proglucagon is processed by PC1/3 to form GLP-1, GLP-2, and glicentin (45). Deletion of the PC1/3 gene produces a complex phenotype of postnatal dwarfism with hyperproinsulinemia and a failure to process proglucagon and insulin (46). Disruption of the PC2 gene caused a delay in islet cell differentiation with a prolonged presence of cells coexpressing glucagon and insulin, a cell phenotype not normally seen after embryonic d 13 of development in mice, or glucagon, Pdx-1, and Nkx6.1 (46, 47). A 3-fold increase in the proliferative rate of proglucagon cells occurred in perinatal life, resulting in adult α-cell hyperplasia. Increased numbers of smaller islets were also found in the pancreas. Deletion of the PC2 gene resulted in hyperplasia of somatostatin cells (47). The PCs in pancreas changed dramatically as a result of hyperglycemia/hypoinsulinemia. When most β-cells in the adult rat were deleted using STZ, a much-increased presence of PC1/3, PC2, glucagon, and GLP-1 was reported after 6 d in the remaining islets, whereas GLP-1 levels were increased in pancreas and serum (48). However, the ratio of proinsulin to insulin was unaltered, and the increase in PC2 expression was limited to α-cells.

The present studies strongly suggest a change in the relative expression of PC1/3 and PC2 within the α-cell population 1–2 wk after STZ treatment. As in the PC2 gene-deleted mouse, we found rapid α-cell hyperplasia with evidence of α-cell immaturity and a greater appearance of locally produced GLP-1. Because circulating GLP-1 was also elevated, the possibility cannot be excluded that altered processing of the proglucagon gene also occurred in intestinal L cells. These findings suggest that a regenerative plasticity of the β-cell population in early life involves an ability to modulate proglucagon gene processing and cell number in the adjacent α-cells, resulting in the increased local availability of GLP-1. Pancreatic GLP-1 was detected in control animals on postnatal d 8 (4 d after STZ) and declined with age until it was barely detectable by 44 d of age. This is not a direct measure of α-cell ontogeny, because substantial acinar cell hyperplasia and hypertrophy occur before weaning in rats, but it indicates that local production of GLP-1 contributes to the

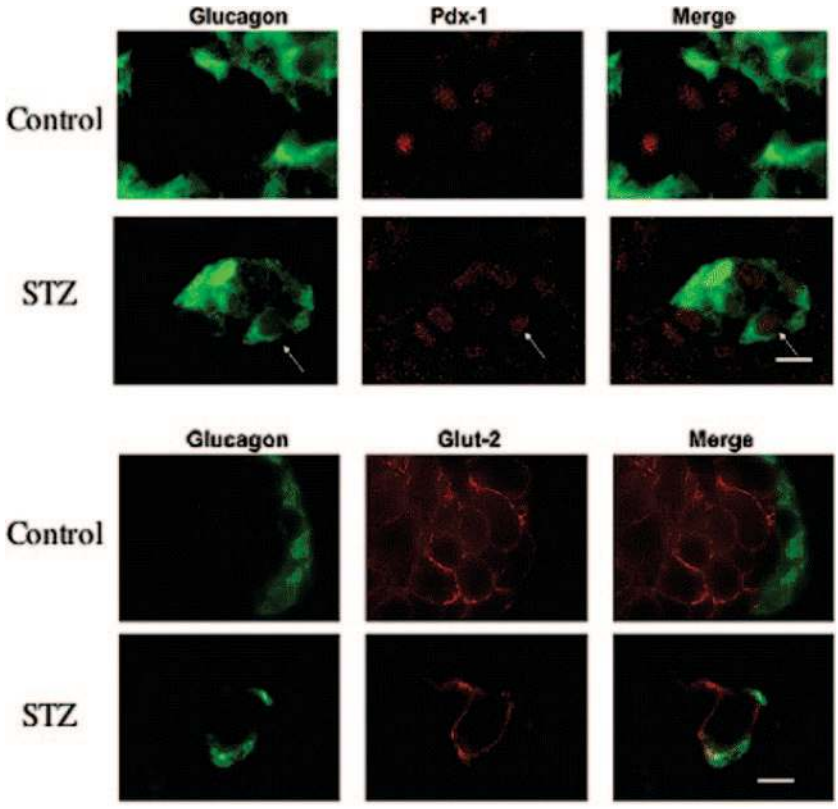

FIG. 12. Immunofluorescent colocalization of glucagon with either Pdx-1 or Glut-2 and their superimposition in the same histological sections from control animals or 8 d after treatment with STZ. Magnification *bar*, 10 μm.

developmental remodeling of the islets seen at this time. The abundance in the rat pancreas of the biologically active and processed amidated form of GLP-1 is maximal on postnatal d 8 (49). This GLP-1 is functionally active, because we found that administration of the GLP-1 receptor antagonist, GLP-1-(9–39), caused a reduction in the recovery of β-cells after STZ and resulted in worse glucose tolerance in these animals. The use of GLP-1-(9–39) was previously shown to be less effective in preventing β-cell recovery after partial pancreatectomy compared with the phenotype in GLP-1 receptor-null mice (50).

The identity of the target cells for GLP-1 action is unclear. This is likely to include remaining differentiated β-cells, because the proliferation rate of insulin-positive cells was increased 8 d after STZ, and expression of GLP-1 receptor was present at this time. However, after STZ treatment, an increased number of atypical insulin-positive cells was found in the core of small and medium-sized islets that colocalized both glucagon and GLP-1 receptor. This may reflect differentiation of new endocrine cells from resident precursors (27) or, possibly, dedifferentiation of existing endocrine cells to a proliferative precursor phenotype and subsequent redifferentiation into β-cells. Similar cells coexpressing insulin and glucagon were also reported after near-total ablation of β-cells with STZ in neonatal rats (51). Dedifferentiation of islet-derived endocrine cells into cytokeratin-positive epithelial cells expressing c-Kit and/or nestin and their expansion over multiple passages have been reported *in vitro* (52–54). These cultures lose expression of all endocrine cell markers, but are able to form pseudoislet structures and reexpress insulin once transferred to a collagen type 4/laminin-rich matrix.

In summary, by inducing β -cell loss with STZ between birth and weaning, we have documented a rapid regeneration that appears to involve the generation of new islets and the restructuring of preexisting islets. Coincident with β -cell renewal within islets was a hyperplasia of glucagon-positive cells and a change in proglucagon gene processing to favor GLP-1. This is likely to reflect a homeostatic stimulus to restore β-cell mass, which may become rate limiting with age.

Acknowledgments

We thank Ms. Brenda Strutt, Ms. Catherine Currie, Becky McGirr, and Mr. Francisco Arany for technical support.

Received April 5, 2005. Accepted February 8, 2006.

Address all correspondence and requests for reprints to: Dr. David J Hill, Lawson Health Research Institute, St. Joseph's Health Care, 268 Grosvenor Street, London, Ontario, Canada N6A 4V2. E-mail: dhill@lri.sjhc.london.on.ca.

This work was supported by the Canadian Institutes of Health Research, the Canadian Diabetes Association, the Juvenile Diabetes Research Foundation, the Stem Cell Network Center of Excellence, and the Ontario Research and Development Challenge Fund.

The authors have no duality of interest with any company whose products or services are directly linked to the subject matter of this paper.

References

1. **Gepts W, de Mey J** 1978 Islet cell survival determined by morphology. An immunocytochemical study of the islet of Langerhans in juvenile diabetes mellitus. Diabetes 27(Suppl 1):251–261

2. **Volk BW, Wellman KF** 1985 The pancreas in idiopathic diabetes. In: Volk BW, Arquilla ER, eds. The diabetic pancreas. 2nd ed. New York: Plenum Press; 353
3. **Hess D, Li L, Sakano S, Hill DJ, Strutt B, Thyssen S, Gray D, Bhatia M** 2003 Bone marrow derived stem cells rescue hyperglycemia by regeneration of recipient islets. Nat Biotechnol 21:763–770
4. **Kodoma S, Kuhtreiber W, Fujimura S, Dale EA, Faustman DL** 2003 Islet regeneration during the reversal of autoimmune diabetes in NOD mice. Science 302:1223–1227
5. **Edlund H** 2001 Developmental biology of the pancreas. Diabetes 50(Suppl 1):S5–S9
6. **Soria B** 2001 In vitro differentiation of pancreatic β-cells. Differentiation 68: 205–219
7. **Habener JF, Kemp DM, Thomas MK** 2005 Minireview: transcriptional regulation in pancreatic development. Endocrinology 146:1025–1034
8. **Scaglia L, Cahill CJ, Finegood DT, Bonner-Weir S** 1997 Apoptosis participates in the remodeling of the endocrine pancreas in the neonatal rat. Endocrinology 138:1736–1741
9. **Petrik J, Arany E, McDonald TJ, Hill DJ** 1998 Apoptosis in the pancreatic islet cells of the neonatal rat is associated with a reduced expression of insulin-like growth factor II that may at as a survival factor. Endocrinology 139:2994–3004
10. **Gu G, Dubauskaite J, Melton DA** 2002 Direct evidence for the pancreatic lineage: $NGN3^+$ cells are islet progenitors and are distinct from duct progenitors. Development 129:2447–2457
11. **Mellitzer G, Martin M, Sidhoum-Jenny M, Orvain C, Barths J, Seymour PA, Sander M, Gradwohl G** 2004 Pancreatic islet progenitor cells in neurogenin 3-yellow fluorescent protein knock-add-on mice. Mol Endocrinol 18:2765–2776
12. **Joanette E, Reusens B, Arany E, Thyssen S, Remacle RC, Hill DJ** 2004 Low protein diet during early life causes a reduction in the number of cells immunopositive for nestin and CD34 in both pancreatic ducts and islets in the rat. Endocrinology 145:3004–3013
13. **Treutelaar MK, Skidmore JM, Dias-Leme CL, Hara M, Zhang L, Simeone D, Martin DM, Burant CF** 2003 Nestin lineage cells contribute to the microvasculature but not endocrine cells of the islet. Diabetes 52:2503–2512
14. **Delacour A, Nepote V, Trumpp A, Herrera PL** 2004 Nestin expression in pancreatic exocrine cell lineages. Mech Dev 121:3–14
15. **Herrera PL** 2002 Defining the cell lineages of the islets of Langerhans using transgenic mice. Int J Dev Biol 46:97–103
16. **Herrera PL** 2000 Adult insulin- and glucagon-producing cells differentiate from two independent cell lineages. Development 127:2317–2322
17. **Fernandes A, King LC, Guz Y, Stein R, Wright CV, Teitelman G** 1997 Differentiation of new insulin-producing cells is induced by injury in adult pancreatic islets. Endocrinology 138:1750–1762
18. **Montanya E, Nacher V, Biarnes M, Soler J** 2000 Linear correlation between β-cell mass and body weight throughout the lifespan in Lewis rats. Diabetes 49:1341–1346
19. **Bonner-Weir S, Deery D, Leahy JL, Weir GC** 1989 Compensatory growth of pancreatic β-cells in adult rats after short-term glucose infusion. Diabetes 38:49–53
20. **Rosenberg L, Duguid WP, Vinik AL** 1989 The effect of cellophane wrapping of the pancreas in the Syrian golden hamster: autoradiographic observations. Pancreas 4:31–37
21. **Prado ML, Cruz AR** 1983 Adaptation of the endocrine tissue of rat pancreas after partial pancreatectomy—a morphometric study. Acta Anat 116:346–352
22. **Portha B, Blondel O, Serradas P, McEvoy R, Giroix MH, Kergoat M, Bailbe D** 1989 The rat models of non-insulin dependent diabetes induced by neonatal streptozotocin. Diabete Metab 15:61–75
23. **Movassat J, Saulnier C, Portha B** 1997 Insulin administration enhances growth of the β-cell mass in streptozotocin-treated newborn rats. Diabetes 46:1445–1452
24. **Bonner-Weir S, Trent DF, Honey RN, Weir GC** 1981 Responses of neonatal rat islets to streptozotocin: limited B-cell regeneration and hyperglycemia. Diabetes 30:64–69
25. **Guz Y, Nasir I, Teitelman G** 2001 Regeneration of pancreatic β-cells from intra-islet precursor cells in an experimental model of diabetes. Endocrinology 142:4956–4968
26. **Dor Y, Brown J, Martinez OI, Melton DA** 2004 Adult pancreatic β-cells are formed by self-duplication rather than stem-cell differentiation. Nature 429: 41–46
27. **Seaberg RM, Smukler S, Kieffer TJ, Enikolopov G, Asghar Z, Wheeler MB, Korbutt G, van der Kooy D** 2004 Clonal identification of multipotent precursors from adult mouse pancreas that generate neural and pancreatic lineages. Nat Biotech 22:1115–1124
28. **Hsu SM, Raine L, Fanger H** 1981 Use of avidin-biotin peroxidase complex (ABC) in immunoperoxidase techniques: a comparison between ABC and unlabelled antibody (PAP) procedures. J Histochem Cytochem 29:577–580
29. **Bock T, Pakkenberg B, Buschard K** 2003 Increased islet volume but unchanged islet number in *ob/ob* mice. Diabetes 52:1716–1722
30. **Bock T, Kynel A, Pakkenberg B, Buschard K** 2003 The postnatal growth of the β-cell mass in pigs. J Endocrinol 179:245–252
31. **Wang R, Li J, Yashpal N** 2004 Phenotypic analysis of c-kit expression in epithelial monolayers derived from postnatal rat pancreatic islets. J Endocrinol 182:113–122
32. **Jensen J, Serup P, Karlsen C, Nielsen TF, Madsen OD** 1996 mRNA profiling of rat islet tumors reveals nkx 6.1 as a β-cell-specific homeodomain transcription factor. J Biol Chem 27:18749–18785
33. **Lindqvist N, Vidal-Sanz M, Hallbook F** 2002 Single cell RT-PCR analysis of tyrosine kinase receptor expression in adult rat retinal ganglion cells isolated by retinal sandwiching. Brain Res Brain Res Protoc 10:75–83
34. **Gelling RW, Du XQ, Dichmann DS, Romer J, Huang H, Cui L, Obici S, Tang B, Holst JJ, Fledelius C, Johansen PB, Rossetti L, Jelicks LA, Serup P, Nishimura E, Charron MJ** 2003 Lower blood glucose, hyperglucagonemia, and pancreatic α cell hyperplasia in glucagon receptor knockout mice. Proc Natl Acad Sci USA 100:1438–1443
35. **Detrillaux MC, Portha B, Roze C, Hollande E** 1982 Ultrastructural study of pancreatic B cell regeneration in newborn rats after destruction by streptozotocin. Virch Arch 39:173–185
36. **Wang RN, Bouwens L.Koppel G** 1994 β Cell proliferation in normal and streptozotocin-treated newborn rats: site, dynamics and capacity. Diabetologia 37:1088–1096
37. **Nagasao J, Yoshioka K, Amasaki H, Mutoh K** 2004 Expression of nestin and IGF-I in rat pancreas after streptozotocin administration. Anat Histol Embryol 33:1–4
38. **Chen L, Komiya I, Inman L, McCorkle K, Alam T, Unger RH** 1989 Molecular and cellular responses of islets during perturbations of glucose homeostasis determined by in situ hybridization histochemistry. Proc Natl Acad Sci USA 86:1367–1371
39. **Raskin P, Aydin I, Unger RH** 1976 Effect of insulin on the exaggerated glucagon response to arginine stimulation in diabetes mellitus. Diabetes 25: 227–229
40. **Vincent M, Guz Y, Rozenberg M, Webb G, Furuta M, Steiner D, Teitelman G** 2003 Abrogation of protein convertase 2 activity results in delayed islet cell differentiation and maturation, increased α-cell proliferation, and islet neogenesis. Endocrinology 144:4061–4069
41. **Stoffers DA** 2004 The development of β-cell mass: recent progress and potential role of GLP-1. Horm Metab Res 36:811–821
42. **Bulotta A, Farilla L, Hui H, Perfetti R** 2004 The role of GLP-1 in the regulation of islet cell mass. Cell Biochem Biophys 40(Suppl 3):65–78
43. **Abraham EJ, Leech CA, Lin JC, Zulewski H, Habener JF** 2002 Insulinotropic hormone glucagon-like peptide-1 differentiation of human pancreatic islet-derived progenitor cells into insulin-producing cells. Endocrinology 143:3152–3161
44. **Dhanvantari S, Seidah NG, Brubaker PL** 1996 Role of prohormone convertases in the tissue specific processing of proglucagon. Mol Endocrinol 10:342–355
45. **Scopsi L, Gullo M, Rilke F, Martin S, Steiner DF** 1995 Pro-protein convertases (PC1/3 and PC2) in normal and neoplastic human tissues: their use as markers of neuroendocrine differentiation. J Clin Endocrinol Metab 80:294–301
46. **Zhu X, Zhou A, Dey A, Norrbom C, Caroll R, Zhang C, Laurent V, Lindberg I, Ugleholdt R, Holst JJ, Steiner DF** 2002 Disruption of PC1/3 expression in mice causes dwarfism and multiple neuroendocrine peptide processing defects. Proc Natl Acad Sci USA 99:10293–10298
47. **Furuta M, Yano H, Zhou A, Rouille Y, Holst JJ, Carroll R, Ravazzola M, Orci L, Furuta H, Steiner DF** 1997 Defective prohormone processing and altered pancreatic islet morphology in mice lacking active SPC2. Proc Natl Acad Sci USA 94:6646–6651
48. **Nie Y, Nakashima M, Brubaker PL, Li QL, Perfetti R, Jansen E, Zambre Y, Pipeleers D, Friedman TC** 2000 Regulation of pancreatic PC1 and PC2 associated with increased glucagon-like peptide 1 in diabetic rats. J Clin Invest 105:955–965
49. **Kreymann B, Ghatei MA, Domin J, Kanse S, Bloom SR** 1991 Developmental patterns of glucagon-like peptide-1-(7–36) amide and peptide-YY in rat pancreas and gut. Endocrinology 129:1001–1005
50. **DeLeon DD, Deng S, Madani R, Ahima RS, Drucker DJ, Stoffers DA** 2003 Role of endogenous glucagon-like peptide-1 in islet regeneration after partial pancreatectomy. Diabetes 52:365–371
51. **Ferrand N, Astesano A, Phan H-H, Lelong C, Rosselin G** 1995 Dynamics of pancreatic cell growth and differentiation during diabetes reversion in STZ-treated newborn rats. Am J Physiol 269:C1250–C1264
52. **Wang R, Li J, Yashpal N, Gao N** 2005 Nestin expression and clonal analysis of islet-derived epithelial monolayers: insight into nestin-expressing cell heterogeneity and differentiation potential. J Endocrinol 184:329–339
53. **Gershengorn MC, Hardikar AA, Wei C, Geras-Raaka E, Marcus-Samuels B, Raaka BM** 2004 Epithelial to mesenchymal transition generates proliferative human islet precursor cells. Science 306:2261–2264
54. **Banerjee M, Bhonde RR** 2003 Islet generation from intra islet precursor cells of diabetic pancreas: In vitro studies depicting in vivo differentiation. J Pancreas 4:137–145

***Endocrinology* is published monthly by The Endocrine Society (http://www.endo-society.org), the foremost professional society serving the endocrine community.**